Polymer Testing 116 (2022) 107796

Contents lists available at ScienceDirect

Polymer Testing

journal homepage: www.elsevier.com/locate/polytest

Polymerization of chondroitin sulfate and its stimulatory effect on cartilage regeneration; a bioactive material for cartilage regeneration

N. Rashidi [a,*], M. Tamaddon [b], C. Liu [b], J. Czernuszka [a]

[a] Department of Materials, University of Oxford, Oxford, OX1 3PH, UK
[b] Institute of Orthopaedic & Musculoskeletal Science, Division of Surgery & Interventional Science, University College London, Royal National Orthopaedic Hospital, Stanmore, HA7 4LP, UK

ARTICLE INFO

Keywords:
Chondroitin sulfate polymerization
Cartilage regeneration
Collagen II -Chondroitin sulfate scaffolds
Higher molecular weight chondroitin sulfate
Cartilage tissue engineering

ABSTRACT

Chondroitin sulfate (CS) is one of the major glycosaminoglycans (GAGs). GAGs are linear polymers comprising disaccharide residues and are found as the side chains of proteoglycans. CS has significant stimulatory effects on cell behavior and is widely used in tissue-engineered and drug delivery devices. However, it is difficult to incorporate a sufficient amount of CS into biopolymer-based scaffolds such as collagen to take full advantage of its benefit. In this study, CS has been polymerized to an 11 times higher molecular weight polymer (PCS) in an attempt to overcome this deficiency. We have previously shown that PCS was significantly more effective than CS in chondrogenesis. This study aimed to characterize the physicochemical properties of the manufactured PCS. PCS was characterized by Fourier transform infra-red (FTIR) spectroscopy together with X-ray photoelectron spectroscopy (XPS) to obtain information about its chemical structure and elemental composition. Its molecular size was measured using dynamic light scattering (DLS) and its viscoelastic properties were determined by rheology measurements. The average PCS diameter increased 5 times by polymerization and PCS has significantly enhanced viscoelastic properties compared to CS. The molecular weight of PCS was calculated from the rheological experiment to give more than an order of magnitude increase over CS molecular weight. Based on these results, we believe there is a great potential for using PCS in regenerative medicine devices.

1. Introduction

Chondroitin sulfate is a key component of the cartilage extracellular matrix (ECM) [1]. It is considered a member of the glycosaminoglycans (GAGs) family and is an unbranched sulfated, highly water-soluble anionic polysaccharide [2]. The chain is composed of sulfated, negatively charged, repeating disaccharides, N-acetylglucosamine or N-acetylgalactosamine and glucuronic acid as the second sugar residue [3] (Fig. 1). CS chains show structural diversity since the sulfate groups can be bound to the different positions on the disaccharide units, and its molecular weight (MW) is also highly variable due to the different numbers of the disaccharide units [4–6]. Its anionic nature enables efficient interaction with cationic molecules and can function as cell interacting molecules [7]. CS has hydroxyl and carboxyl groups on its backbone, thus allowing the introduction of other functional groups [8,9]. Modification of CS with various functional groups makes this biomacromolecule suitable for different pharmaceutical or tissue engineering applications [10].

It has been shown that the incorporation of CS in scaffolds for cartilage tissue engineering induces the chondrogenic differentiation of mesenchymal stem cells (MSCs) [11–13]. CS provides a microenvironment that enhances clustering of cells (pre-cartilage condensation of mesenchymal cells), upregulates cartilage-specific genes, and provides cell-mediated degradable sites for the cell clusters to grow further and produce ECM [14]. Studies have also demonstrated that CS increases the compressive stiffness of collagen scaffolds [15].

Despite these advantages, there has been a challenge in incorporating CS into biopolymer-based scaffolds such as collagen. There are limited binding sites on a collagen molecule for CS attachment - carboxyl groups of CS attach to amine groups of collagen. Moreover, CS is water-soluble and dissolves rapidly in a cell culture medium [16,17]. We aimed to address these problems by polymerizing CS. There are a number of studies on the synthesis of oligo- and poly-saccharides by chemical [18–22] and enzymatic methods [23-25]. There are also patents on producing water-insoluble polysaccharides by using a cross-linking agent [26] and/or by polycondensation of saccharides in

* Corresponding author.
E-mail address: n.rashidi@ucl.ac.uk (N. Rashidi).

https://doi.org/10.1016/j.polymertesting.2022.107796
Received 23 May 2022; Received in revised form 12 September 2022; Accepted 14 September 2022
Available online 15 September 2022

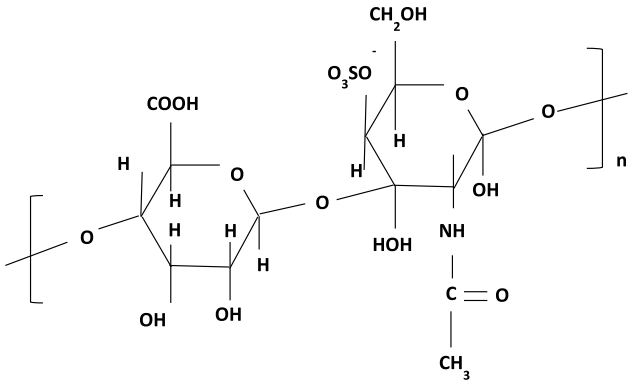

Fig. 1. Chondroitin sulfate chemical structure; carboxylic (-COOH) and carbonyl (-C-O-) groups are involved in the polymerization process. The carboxylic group is also the binding site for the attachment to another biopolymer such as collagen.

the presence of carboxylic acid catalysts at reduced pressure [27].

From the existing methods for polymerization of a saccharide, two chemical methods (solid-state polycondensation and polycondensation in aqueous media) were selected. Solid-state polycondensation which is also called powder to powder polycondensation or anhydrous melt polymerization is a method used for the polymerization of natural saccharides. The reaction is found to take place in the presence of a catalyst (P_2O_5) under reduced pressure (or under nitrogen flow) [28]. However, our preliminary study showed that this method leads to oxidization of CS and is hence not suited to its polymerization (data not shown).

Polycondensation of natural saccharides is another method, in which saccharides are heated above their melting points in the presence of acid catalysts to produce branched polysaccharides [28]. In this study, we adopted the polycondensation method with some modifications to polymerize CS and increase not only its incorporation but also its stability within a collagenous scaffold. The main advantages of this method are its simplicity, the production of a biocompatible polymer (PCS) with desirable characteristics, good conversion of CS to PCS, and the ease of separation of PCS from the medium (the water-insoluble PCS is extracted easily from the medium by centrifugation).

We show here that PCS can further increase the viscoelastic properties of scaffolds which leads to an increase in the scaffolds' stiffness and biostability after implantation. More importantly, we have shown previously that PCS upregulates the expression of chondrogenic markers of sheep bone marrow mesenchymal stem cells (MSCs) [29]. This could be a major advance in tissue engineering of cartilage tissue.

2. Materials and method

2.1. Polymerization of chondroitin sulfate

Chondroitin 4-sulfate extracted from the bovine trachea (Sigma Aldrich, UK) was polymerized based on the modification of a protocol used for crosslinking of saccharides (polycondensation of natural saccharides) [30], in which saccharides are heated above their melting points in the presence of acid catalysts to produce branched polysaccharides.

The chain length polycondensation/chain crosslinking was conducted by heating CS in deionized water in the presence of phosphoric acid (Sigma Aldrich, UK) as a catalyst. To obtain the highest amounts of PCS in the form of precipitate, the proportions of acid, water, and CS were varied. The baseline reaction temperature was 150 °C following the reaction temperature range offered for the polymerization of saccharides [31]. After several iterations, the optimum amount of reagents with the least reaction duration (3 h) and the highest product yield was found to be 5 g CS, 150 ml water, and 0.1 ml phosphoric acid at 150 °C. Briefly, 5 g CS was stirred in 150 ml distilled water until completely dissolved and 0.1 ml phosphoric acid was added to the CS solution. The solution was then covered up with an aluminum foil to prevent water loss throughout the reaction and then heated up to 150 °C on a hot plate. The precipitate (PCS) was formed after 3 h and separated from the solution by centrifugation (Thermo Scientific, CL10 centrifuge) at 3000 rpm for 5 min. The precipitate was then washed with deionized water, frozen at −20C (Zanussi, DF 50/16), and freeze-dried (Christ Alpha 1–5).

2.2. Fourier transform infra-red spectroscopy (FTIR)

The samples were analyzed in the absorbance mode at 4 cm^{-1} resolution 64 times over the range of 500–4000 cm using an Agilent FTS 3500 Excalibur. The FTIR spectra of CS and PCS were normalized against the C–H stretch band by dividing the intensity of each band to the intensity of the C–H band which remains unchanged by polymerization. To separate the overlapping peaks, second derivative spectroscopy was used by deconvolution in Origin Pro 9.1 software. Here, the registered raw spectrum is numerically differentiated twice.

2.3. X-ray photoelectron spectroscopy (XPS)

Samples were analyzed using a Thermo Scientific K-alpha XPS instrument equipped with a micro-focused monochromated Al X-ray source. The source was operated at 12 keV and a 400-μm spot size was used. The analyzer operates at constant analyzer energy (CAE) of 200 eV for survey scans and 50eV for detailed scans. Charge neutralization was applied using a combined low energy/ion flood source. The data acquisition and analysis were performed with Thermo Scientifics Avantage software. Peak fitting (Lorentzian/Gaussian (L/G) 30%) was applied following the removal of a Smart background. Normalized atomic percentages were determined from peak areas of the elemental main peaks detected on the survey scan following background subtraction and application of Thermo sensitivity factors.

2.4. Dynamic light scattering (DLS)

The particle size of chondroitin sulfate (CS) and polymerized chondroitin sulfate (PCS) was measured by a Malvern ZetaSizer Nano ZS (size range: 0.3 nm to 10 μm). To obtain the average diameter, a cuvette was filled with 1 ml of the CS solution/PCS dispersion in water (1% w/v) and inserted into the instrument. 5 measurements were performed and the mean particle size was calculated.

2.5. Rheological measurements

Rheological tests in two different conditions were performed on the CS solution and PCS dispersion using an Anton Paar 301. First, to obtain the viscosities of CS and PCS, an oscillatory shear test was conducted. The polymer solution/dispersion was prepared by dissolution of CS/dispersion of PCS in 0.2 M NaCl solution. The dynamic viscosity of CS and PCS preparations at the constant shear rate of 100/s and the temperature of 25 °C was measured using a flat plate (50 mm diameter) and a gap size of 1 mm between the cylinder head and the base.

Second, the viscoelastic properties of the preparations, including storage modulus (G'), loss modulus(G"), complex modulus (G*), and complex viscosity (η*) were determined using an oscillatory frequency sweep test within LVR, at 1% strain with an angular frequency of 0.1–100% and the temperature of 20 °C. A flat plate (50 mm diameter) was used and the gap size of 1 mm was set between the cylinder head and the base.

2.6. Scaffold fabrication

Type-II collagen was extracted from fetal bovine articular cartilage

using a limited pepsin digest followed by differential salt fractionation [32]. 1% (w/v) pure afibrillar collagen suspension was produced by adding lyophilized collagen monomers to dilute acetic acid (pH 3.2). The preparation was then homogenized in an ice bath to reduce the denaturation of collagen. The dispersion was then degassed using centrifugation and was induced to self-assemble, at a 1:1 vol ratio, in tris-buffered saline (TBS) (Sigma Aldrich, UK) solution in the pH of 7.5 in an incubator at 37 °C for 2 h. CS/PCS was then added to the collagen suspension and were crosslinked to collagen fibrils using 60 mm ethyl-3-(3-dimethyl aminopropyl)-carbodiimide (EDC) and 30 mm N-hydroxysuccinimide (NHS) (Sigma Aldrich, UK). The mixture was crosslinked for 3 h. To remove crosslinking reagents, the suspension was then centrifuged for 5 min. Collagen pellet was collected from the centrifuge tube and transferred to a beaker to wash twice in 400 ml Na2HPO4 (0.1 m) for 2 h and twice in 400 ml deionized water for 1 h.

Collagen suspension was injected into the prepared cylindrical polytetrafluoroethylene (PTFE) molds (sealed at one end, with a diameter of 0.8 cm and length of 1.2 cm) and frozen at −20 °C and freeze-dried (Christ Alpha 1–5) for 24 h.

2.6.1. Scaffold characterization

The collagen suspension viscosity was measured using an Anton Paar 301 rheometer in oscillatory frequency mode (angular frequency = 0.1–1001 s^{-1}, amplitude = 1%, at 20 °C). The compressive moduli of scaffolds were measured using Zwick Mechanical equipped with a 5 N cell load operated at the crosshead speed of 5 mm/min. All compression tests were conducted perpendicular to the plane of the scaffold disc in a dry state. The compressive moduli of scaffolds were obtained as the slope of the linear region of stress-strain curves. The relative densities of the scaffolds were determined by dividing the density of the scaffolds to the density of solid material (ρ_{col} = 1.3 g/cm^3, ρ_{CS} = 5.5 g/cm^3, ρ_{PCS} = 12.1 g/cm^3). The scaffold's densities were calculated by measuring the weight and dimensions of the scaffolds.

2.7. Statistical analysis

Analysis of variance (ANOVA) tests was performed in SPSS for each test. All post hoc tests were Bonferroni corrected for multiple comparisons. Significance was accepted at a level of 0.05. If sphericity was violated, Greenhouse Geiser correction values for ANOVA are reported. The sample numbers for FTIR, XPS, DLS, and rheology measurements were n = 3 and for mechanical testing n = 5.

3. Results

3.1. Fourier transform infra-red spectroscopy (FTIR)

FTIR spectroscopy has been conducted on CS and PCS to examine any possible peak shifts or new bond formation in the PCS spectrum (Fig. 2 a and b). The FTIR spectra of CS and PCS were normalized against the C–H stretch band (Fig. 2a) which remains unchanged by polymerization. The FTIR spectrum of CS exhibits O–H and N–H stretching (amide A) vibrations at 3321 cm^{-1} in which the O–H stretching vibration is overlapped by N–H stretching; the C–H stretching of methyl or methylene group at 2925 cm^{-1}; the stretch vibrations of C–O at 1020 cm^{-1}; the band at 1602 cm^{-1} corresponding to amide I, amide II and carboxylate which are overlapped (these peaks are decomposed by deconvolution in Origin Pro 9.1 software (Fig. 2b); the band at 1406 corresponding to C–O stretch vibration; the peak at 1220 cm^{-1} corresponding to the stretching vibrations of S═O bond (SO_4^{2-}) (which is used as a characteristic peak of CS) [33]. These bands are all present in the FTIR spectrum for PCS with a shift in wavenumbers (Table 1). Amide A, amide I, and amide II bands were downshifted to 3315, 1595, and 1525 cm^{-1} in PCS which indicates weaker N–H bonds in PCS.

The carboxylate band shifted to a higher wavenumber of 1736 cm^{-1} signifying that the C═O bond is stronger/shorter in PCS than CS. The S═O, C–O, C–O–C, and C–O–S stretching bands did not change significantly.

The PCS spectra exhibit all the peaks existing in the CS spectra suggesting that the CS backbone structure has not changed due to the polymerization process. The second derivative spectra of PCS (Fig. 2b) depict a band associated with the C═O stretch at 1735 cm^{-1}. The shift in the peak position of the C═O band (corresponding to an ester bond) and the increase in its intensity as well as the increase in the peak intensity of

Table 1
FTIR band assignment for CS and PCS.

Band Assignment	Wave number (cm^{-1})	
	CS	PCS
Amide A (N–H stretching)	3321	3315
C–H stretching	2912	2922
Amide I (C = O stretching)	1604	1595
Amide II (C–N stretching, N–H bending)	1552	1525
COO^- (Ester bond)	1728	1736
C–O stretching	1406	1411
O–H bending	1370	1309
S = O stretching	1220	1224
C– O–C stretching	1018	1020
C–O–S stretching	850	852

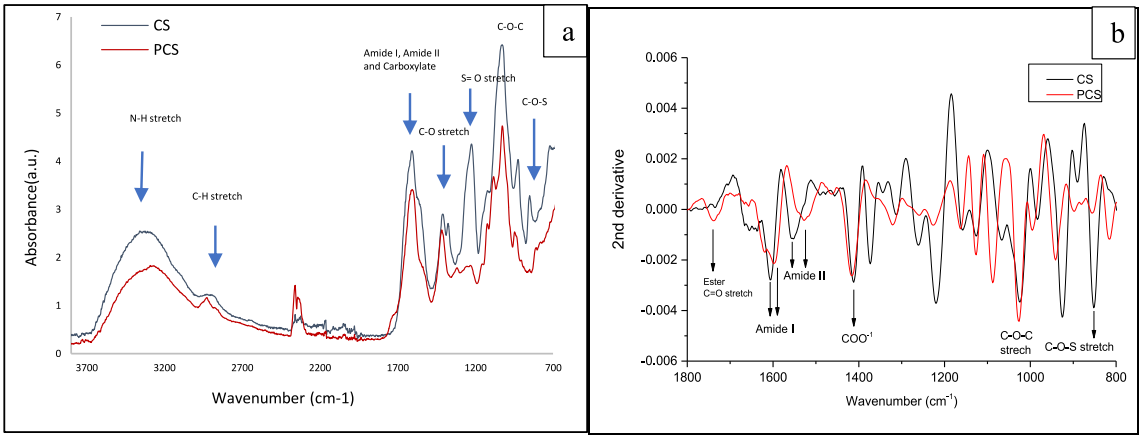

Fig. 2. (a) FTIR spectra of CS and PCS (n = 3), spectra normalized against C–H band. (b) Second derivative FTIR bands of CS and PCS. The peak shift to higher wavenumbers and the increase in peak intensity for C═O and C–O–C bond both indicate the occurrence of polymerization in PCS.

the C–O–C band strongly suggests the occurrence of polymerization.

3.2. X-ray photoelectron spectroscopy

The chemical composition of CS and PCS was further characterized by X-ray photoelectron spectroscopy (XPS). Survey scans of sample powders identified peaks corresponding to C1s (286 eV), O1s (532 eV), and N1s (400 eV) as the main constituents of CS and PCS (Fig. 3a). The presence of sodium in the spectra could be due to the use of chondroitin 4-sulfate sodium.

Table 2 shows that the atomic percentage of carbon significantly increased for PCS, whereas oxygen and sodium percentages slightly decreased. C (1s) peak analysis of PCS and CS (Fig. 3b) showed a higher concentration of COO^- (ester bond) and C–O. This result is consistent with the FTIR data, providing further evidence for the polymerization of CS by either the formation of an ester bond (side branches) or along the polymer chain (chain length polymerization).

3.3. Increase in the average size of CS by polymerization

Dynamic light scattering (DLS) was performed to measure the average diameter of CS and PCS in deionized water. The average diameter of CS and PCS were found to be 551 and 2871 nm respectively (Table 3). The average PCS size significantly ($P < 0.05$) increased by polymerization (5.2 times). These results together with FTIR and XPS confirmed the occurrence of polymerization.

3.4. Molecular weight measurement of PCS based on rheology test

The molecular weight of PCS was obtained based on the viscosity of the polymer and using the Mark -Houwink equation (Equation (4)). The dynamic viscosity of CS and PCS preparations at the constant shear rate of 100/s was measured. For a polymer at low concentrations, it can be assumed that the intrinsic viscosity equals the inherent viscosity [34] (Equation (1)).

$$\eta = \lim_{C\to 0} \frac{\eta_i}{C} = \lim_{C\to 0} \eta_{inh} \quad (1)$$

To identify a sufficiently low concentration at which inherent and intrinsic viscosity can be assumed to be equal, the dynamic viscosity of CS at different concentrations was measured (Fig. 4a). There is a linear relationship between viscosity and concentration at concentrations higher than 0.1 (g/ml), yet viscosity remains relatively constant at concentrations lower than 0.05. The concentration (C) of 0.01 (g/ml) was taken to be sufficiently dilute to allow the use of Equation (1). Therefore, the solutions of CS and PCS with a concentration of 0.01 were prepared for the rheology test. The dynamic viscosity results are presented in Fig. 4b.

Having known the dynamic viscosity of CS, PCS, and the solvent (0.2 M NaCl, measured with a rheometer), the relative viscosity of both polymers can be calculated using Equation (2).

$$\eta_{relative} = (\eta_{\ dynamic})_{CS} / (\eta_{dynamic})_{solvent} \quad (2)$$

The intrinsic viscosity is then calculated using Equation (3):

$$\eta_{intrinsic} = \eta_{inherent} = \ln(\eta_{relative})/C \quad (3)$$

Where C is the concentration.

The Mark-Houwink equation relates the intrinsic viscosity of a polymer (η) to its molecular weight (M).

$$\eta_{intrinsic} = KM^a \quad (4)$$

K and *a* are the Mark-Houwink constants that depend on the polymer−solvent system, temperature, and polymer conformation [35]. The exponent, is a function of the three-dimensional configuration of a polymer chain in a solvent and ranges from 0 to 2. Values range from 0 to 0.5 imply a rigid sphere in an ideal solvent, between 0.5 and 0.8 corresponds to a random coil, and from 0.8 to 2 infers rigid or rod-like polymers (stiff chain). Equation (5) represents the Mark-Houwink parameters of chondroitin sulfate in 0.2 M NaCl at 25 °C indicating that the chondroitin sulfate molecules assume a stiff rod [36].

$$[\eta]\ (cm^3/g) = 1.7 \times 10^{-5}\ M_w^{1.01} \quad (5)$$

The ratio of the Mark-Houwink equation for PCS and CS is (assuming the same *a* for CS and PCS):

$$\eta_{pcs\ /}\ \eta_{cs} = (M_{pcs}/\ M_{cs})^{\ a} \quad (6)$$

The ratio of CS and PCS intrinsic viscosities obtained from Table 4 is 11.45. The molecular weight of CS is given as 20kD by the supplier (Sigma Aldrich, UK), in which case the molecular weight of PCS is 230

Table 2
XPS atomic analysis of CS and PCS (n = 3); a significant increase in C1s for PCS.

Name	Peak center (eV)	CS atomic %	PCS atomic %
O1s	532.7	39.85	34.84
C1s	286.9	46.7	55.64
Na1s	1071.9	4.82	1.66
N1s	400.18	5.7	5.76
S2p	169.32	2.9	2.05

Table 3
Average particle diameter for CS and PCS; a significant increase in PCS diameter.

Sample Name	Average Diameter (nm)
CS	551 ± 125
PCS	2871 ± 494

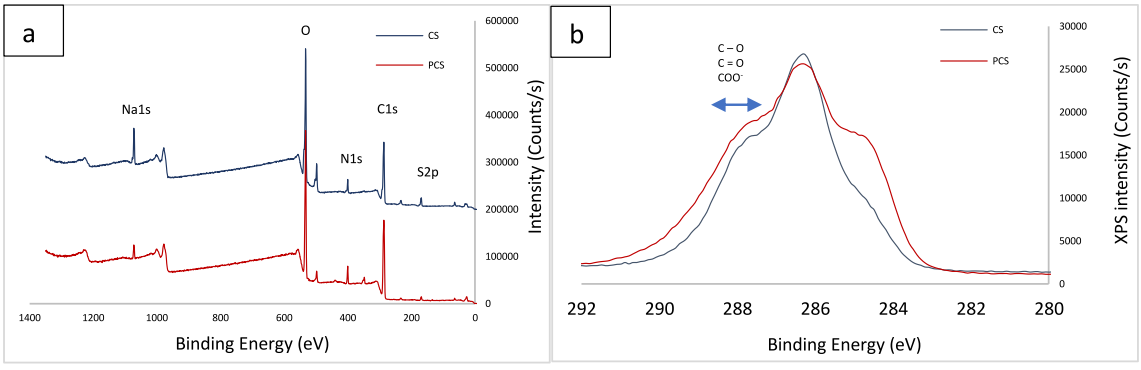

Fig. 3. (a) Survey scan XPS spectra of CS and PCS (n = 3). (b) The C (1s) XPS regions of PCS and CS; a higher concentration of COO^- (ester bond) and C–O for PCS support polymerization has occurred.

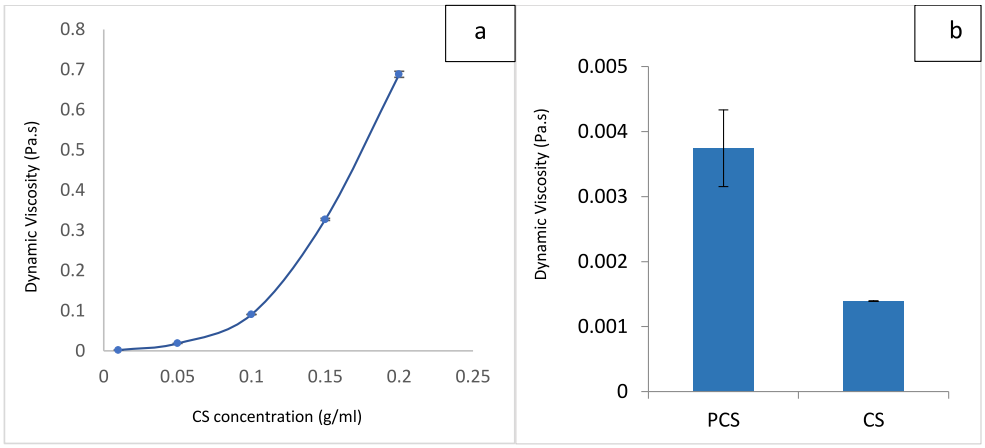

Fig. 4. (a) Dynamic viscosity of CS at concentrations 0.01–0.2 g/mol (shear rate = 100 s^{-1}). (b) Dynamic viscosity of CS and PCS at concentration of 0.01 (g/ml) and shear rate of 100 s^{-1}. Error bars are standard deviations.

Table 4
Dynamic, relative, and intrinsic viscosity of a very dilute solution (C = 0.01 g/ml) of CS and PCS.

Sample Name	$\eta_{dynamic}$ (Pa.s)	$\eta_{relative}$	$\eta_{intrinsic}$
PCS	0.003744 ± 0.0011	2.948	108.11
CS	0.00134 ± 6.32*10^{-6}	1.096	9.21
NaCl	0.00127 ± 2.9*10^{-6}		

KDa.

The molecular weight of PCS can also be obtained using the Einstein viscosity relation [33](Equation (7)), the hydrodynamic radius (r_{pcs}, r_{cs}) obtained by DLS (Table 3) and Equation (8) is derived by dividing the Einstein viscosity equation of PCS to that of CS.

$$\eta = 2.5\ N\ V_e\ /M \tag{7}$$

Where η = viscosity of polymer solution, M = polymer molecular weight (g/mol), N = Avogadro's number, and Ve = the volume of an equivalent spherical particle (cm^3).

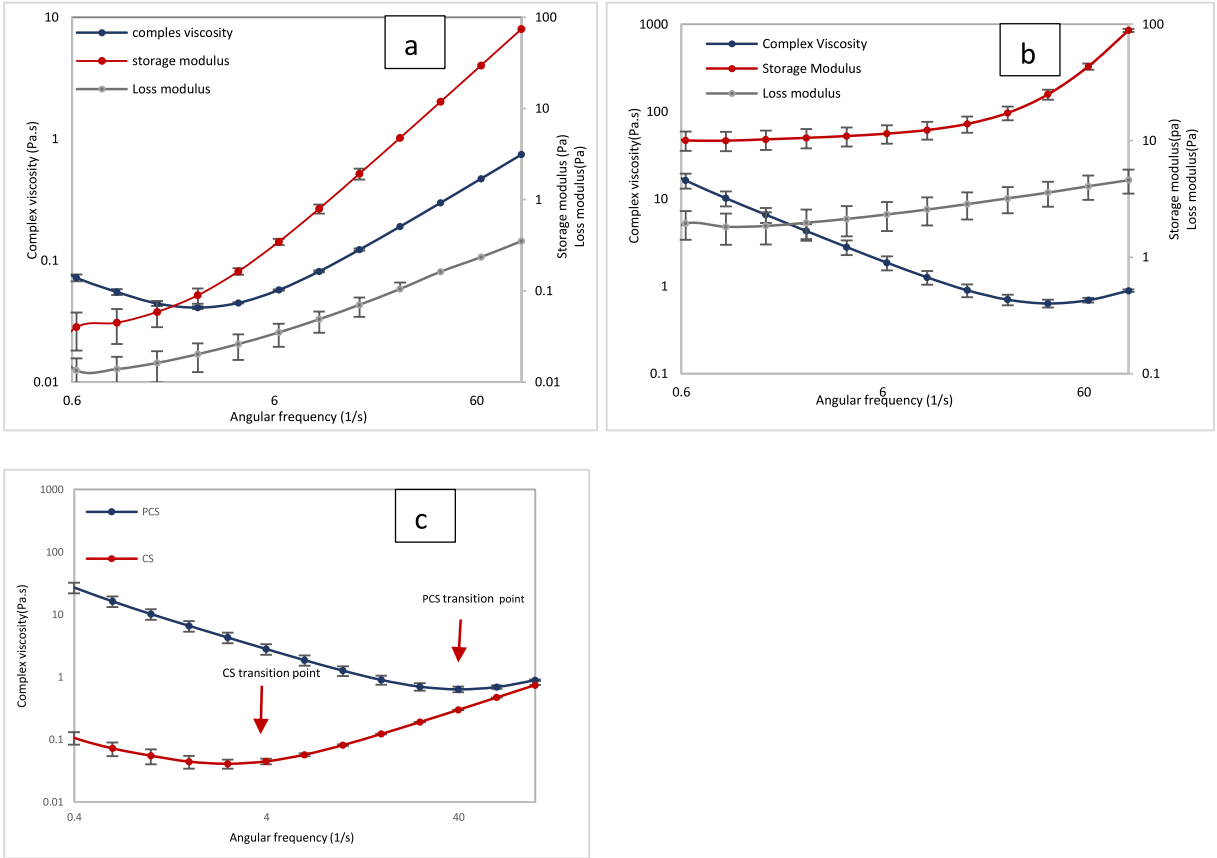

Fig. 5. (a) Complex viscosity, storage and loss modulus of CS solution. (b) Complex viscosity, storage and loss modulus of PCS solution.(c)Transition between shear thinning and shear thickening behavior in CS and PCS. Error bars are standard deviations.

$$M_{pcs}/ M_{cs} = (\eta_{cs}/\eta_{pcs}) (r_{pcs}/ r_{cs})^3 \quad (8)$$

This gives the molecular weight ratio of PCS: CS to be 11.97, which is very similar to the ratio obtained by the Mark- Houwink equation, which was 11.45.

3.5. Viscoelastic behavior of CS and PCS

We investigated the effect of polymerization on the viscoelastic properties of CS by conducting a dynamic frequency sweep test. As shown in Fig. 5a, at a low angular frequency (<2.5 s^{-1}), the complex viscosity of CS decreases by increasing the angular frequency which represents a shear-thinning property. However, at a higher angular frequency (between 2.5 and 100 s^{-1}) the complex viscosity increases by increasing the angular frequency signifying a shear thickening property. PCS has also a shear-thinning property at frequencies less than 40 s^{-1} and a shear thickening property at higher frequencies (Fig. 5b). PCS has a shear thinning property over a more extended range of frequencies compared to CS and the transition between shear thinning and shear thickening occurred at a higher angular frequency for PCS (Fig. 5c).

CS and PCS showed different viscous (loss modulus) and elastic (storage modulus) responses by increasing the angular frequency. The storage (G') and loss modulus (G") of CS substantially increases with the increase in angular frequency while the increase in storage modulus is more prominent. The storage modulus of PCS is constant at the angular frequencies lower than 25 s^{-1} and increases at high angular frequency, but the loss modulus is approximately constant over the whole range of frequency. They both have a higher storage modulus than loss modulus which indicates that their elastic characteristic is dominant. The complex viscosity of PCS is higher than that of CS providing further evidence that PCS has a higher molecular weight (Fig. 5c). Furthermore, the storage and loss modulus of PCS are significantly greater than CS ($P < 0.05$). Yet, the increase in loss modulus of PCS versus CS is much higher than the increase in its storage modulus. In other words, the viscous component is greatly increased by polymerization.

4. The application of PCS in collagen scaffolds for cartilage regeneration

We investigated the effect of PCS introduction on the viscosity of collagen suspensions and scaffolds' compressive stiffness. The viscosity helps to explain the scaffold microstructure and the subsequent mechanical and cellular response. 3 types of collagen II dispersions (XCol2, XCol2-CS, and XCol2-PCS) were prepared (Table 5) and their response to increasing frequency was examined at a constant strain and temperature. Dynamic frequency sweeps were conducted within the Linear Viscoelastic Region (LVR) at 1% strain with 1–100% angular frequency [15].

As shown in Fig. 6a, the viscosity of all the dispersions decreased by increasing angular frequency and exhibited shear thinning, hence they can be categorized as pseudoplastic materials.

XColl2 – PCS has a significantly higher ($P < 0.05$) viscosity than the pure collagen dispersion in the whole range of angular frequency, whereas XColl2 – CS has a lower complex viscosity compared to pure collagen solution. The average complex viscosity, storage, loss and complex moduli are the highest for XColl2- PCS as compared to the other dispersions. Thus, the introduction of PCS to collagen increased the viscoelastic properties of suspensions, yet the addition of CS to collagen reduced the viscoelastic properties. Comparing the characteristics of the scaffolds (Table 5), XCol2-PCS also provides a significantly higher ($P < 0.05$) compressive modulus in relation to XCol2, XCol2-CS.

Table 5
Scaffolds acronyms and their biological and physical characteristics; PCS significantly ($P < 0.05$) increased relative density, specific surface area, and compressive modulus of the collagen scaffold.

Scaffolds Acronyms	Relative density (ρ^*/ρ_s)	Specific surface area (1/μm)	Compressive modulus (KPa)
XColl2-PCS	0.017	0.48	46.4
XColl2-CS	0.0129	0.41	28.4
XColl2	0.013	0.41	8.5

5. Discussion

In this work, a higher molecular weight chondroitin sulfate (PCS) was successfully produced and characterized. The occurrence of the polymerization was confirmed by the analysis of the chemical structure of CS and PCS using FTIR and XPS techniques. Rheology and DLS further supported the occurrence of polymerization by showing the increase in the complex viscosity and the size of PCS. Rheology and DLS data were used separately to obtain PCS's molecular weight and showed a similar molecular weight.

FTIR and XPS outcomes helped us understand the mechanism of polymerization. There are two possible routes for polymerization of CS considering the chemical structure of CS (Fig. 1): 1. Chain length polymerization along the polymer chain (intramolecularly); 2. Formation of side branches through the carboxylic group (intermolecularly).

The first route, polymerization along the CS chain (Fig. 7a), is a polycondensation process in which an anomeric hydroxyl group is activated by phosphoric acid to produce a carbocation, then chain addition can take place intramolecularly (along the polymer chain) or intermolecularly (via carboxylic group route) [28].

Polymerization along the CS chain would create an ether group (-C-O-C-). The increase in the intensity of the ether band by 1.4 times in the PCS FTIR spectrum indicates the polymerization along the polymer chain. This route of polymerization is further confirmed by the XPS results.

The second polymerization route occurs intermolecularly via the carboxylic group route (Fig. 7b). The second derivative spectra of PCS (Fig. 2b) showed an infrared band associated with the C═O stretch at 1735 cm^{-1}. The significant increase in the peak intensity of the ester band suggests that polymerization has occurred through the carboxylic group to form side branches in PCS. XPS results are also in agreement with the FTIR results in which C (1s) peak analysis of PCS and CS (Fig. 3b) showed a higher concentration of the ester and the ether bond for PCS; this further supports the polymerization of CS by the formation of side branches or polycondensation.

It appears from these data that both polymerization mechanisms can occur, the nature of the polymerization route is investigated further via rheology in the following. The complex viscosity of PCS is significantly greater than that of CS at the low angular frequency in which they both exhibit shear-thinning (Fig. 5c). However, at angular frequencies higher than 2.5/s, CS represents shear thickening behavior and its viscosity converges to PCS viscosity at the angular frequencies greater than 60/s. The PCS viscosity is then reduced significantly by increasing the angular frequency, however, the magnitude of decrease in viscosity of PCS during thinning is much greater than the viscosity increase during thickening. In contrast, the magnitude of decrease in viscosity of CS during thinning is considerably less than the rise in viscosity during thickening.

Polymers with high molecular weight are likely to be entangled and randomly oriented when they are at rest. Under shear, they begin to disentangle and align which causes a reduction in viscosity [37]. PCS showed shear-thinning behavior over a broader range of angular frequency compared to CS. It has been suggested that a linear molecule under shear elongates and forms a prolate ellipsoid configuration, whereas a branched molecule flattens and forms an oblate ellipsoid. Moreover, it has been observed that the increase in alignment occurs more intensely for a linear molecule rather than a branched molecule [38]. This suggests that PCS has a branched configuration and could explain why PCS had shear thinning behavior over a broader range of frequency compared to CS. Besides, PCS showed an approximately

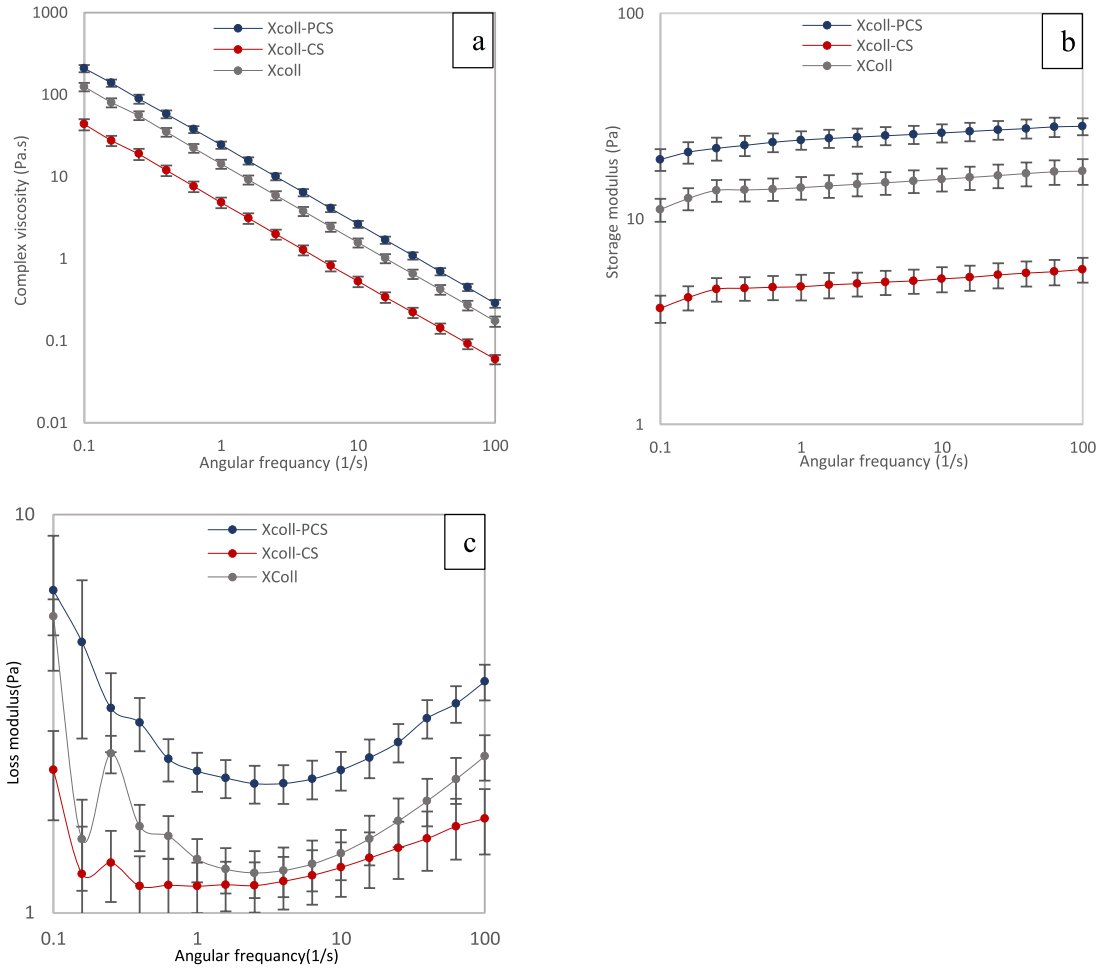

Fig. 6. Complex viscosity, storage and loss moduli of collagen II, collagen II-PCS and collagen II-CS solutions in oscillatory shear test; frequency sweep (angular frequency = 100–0.1 rad/s, strain amplitude γ = 1%, T = 20C). The addition of PCS in collagen type II dispersion increased complex viscosity, storage, and loss moduli. Error bars are standard deviations.

constant storage modulus over a broad range of frequencies. The region of constant G′ is identified as the plateau modulus and implies that little relaxation occurs in this range of frequencies (relaxing back to an equilibrium orientation and configuration following the removal of stress). The relaxation is hindered by the entanglements [39]. As the molecular weight of the polymers increases, the range of frequencies over which G′ is independent of frequency increases [40], reflecting the larger number of entanglements per chain and the more hindered relaxation process. PCS showed a considerably broader region of constant G' compared to CS (Fig. 5a and b), this provides further evidence that PCS has higher molecular weight or it has a longer chain and or more side branches compared to CS.

The parameters that give rise to the difference in PCS and CS rheology are polymer-solvent and polymer-polymer interactions. CS is soluble in water, however, PCS is not water-soluble. The interaction between polymer and solvent affects the configuration of the polymer in solvent. The polymer size (radius of gyration), its molecular weight, and the concentration of polymer solution/suspension influence the interactions between polymer chains in the form of entanglements. We speculate that PCS are highly entwined polymer networks due to the length, configuration (branched polymer), and molecular weight, so the dynamics of chains will be greatly hindered by entanglements. CS could be less entangled due to the linearity of chains, lower molecular weight and size, and higher interaction with the solvent. These are the main factors that contribute to the different rheological behavior of CS and PCS.

Our results showed that the rheological behavior of PCS resembles a gel-like behavior which makes it a perfect choice for hydrogel and tissue engineering applications. The major difference between a gel and a concentrated polymer solution is the existence of bonds between the polymer molecules in a gel rather than just entanglements. Gels commonly show more elastic behavior than polymer solutions at the same concentration since chemical bonds are stronger than physical entanglements [37]. The number of bonds in gels affects its strength and elasticity; as the number of bonds increases the gel elastic modulus increases. In polymer solutions, molecules can entirely disentangle from one conformation and diffuse into another. However, the presence of bonds in the gel network restricts the molecule's movement or relaxation, resulting in a great increase in the relaxation times of the system. It is speculated that there are likely more hydrogen bonds between PCS molecules than CS which makes PCS to more likely behave as a gel. Most importantly, the storage modulus G′ of PCS is independent of frequency over a broad range. This constant storage modulus indicates that there is a little relaxation occurring over these frequencies and PCS is acting like an elastic solid/gel. Second, the loss modulus, G″, is approximately 6 times smaller than the storage modulus. This substantial difference in the magnitude of these two moduli is further evidence that PCS acts like a strong gel and its rheology is dominated by the elastic contribution. The difference in PCS and CS size gives rise to the difference in the onset of shear thickening.; the critical shear rate increased for PCS as the polymer size increased. The onset of transition to shear thickening is commonly characterized by the critical shear rate, or critical shear

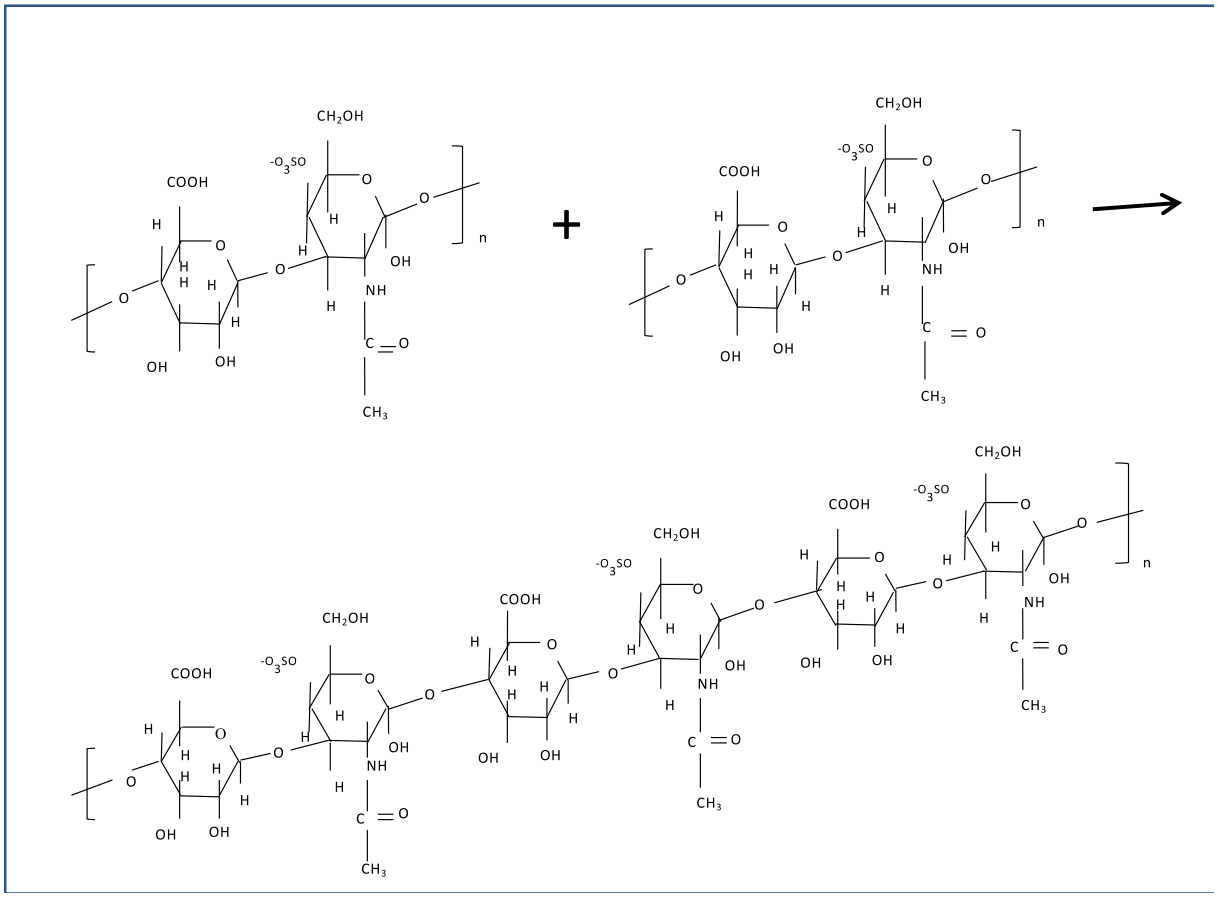

Fig. 7a. Intramolecular chain growth (chain length polymerization).

stress, and can vary significantly between systems. The shear rate at which these transitions occur and the magnitude of the viscosity increase are determined by several factors, including particle concentration, size, shape, size distribution, and inter-particle interactions [41].

We were able to obtain the MW based on the rheology measurements. DLS was also used to measure the PCS and CS size and to calculate the MW accordingly and both methods provided a similar MW. There are a few conventional methods for measuring the molecular weight of a polymer including gel permeation chromatography (GPC), matrix-assisted laser desorption/ionization (MALDI) mass spectroscopy, and Dynamic Light Scattering (DLS) [41–43]. GPC and MALDI mass spec were not informative for obtaining PCS molecular weight probably due to its high MW.

We investigated the effect of PCS introduction on the rheological and mechanical characteristics of collagen-based scaffolds. XCol2-PCS provides a significantly higher compressive modulus in relation to XCol2 and XCol2-CS. It can be said that the higher relative density gives rise to the higher modulus of XColl2-PCS. Scaffold stiffness has been shown to regulate cellular behavior (adhesion and ingrowth) and affect stem cell differentiation [44,45]. In this work, Young's modulus of scaffolds was increased one order of magnitude by collagen crosslinking compared to previous work which had only used non-crosslinked collagens [15].

XColl2-PCS has a higher specific surface area and compressive modulus than those of XColl2-CS and XColl2. This gives rise to its higher cell attachment and proliferation which was shown in our previous research [29]. XColl2-CS and XColl2 have the same specific surface area, while XColl2-CS compressive modulus is significantly higher than XColl2. Thus, its higher cell attachment and proliferation stems from either its greater compressive modulus or its composition. We have also previously shown that XColl2- PCS significantly increased the expressions of Coll2 (10 times) and aggrecan (3.2 times) as compared to XColl2- CS which is a huge enhancement toward chondrogenic lineage [29].

6. Conclusion

A higher molecular weight chondroitin sulfate (PCS) was successfully produced. Rheology experiments revealed that the molecular weight of PCS is 11.45 times greater than that of CS. Rheological analysis of PCS and CS showed that PCS possesses a higher viscosity, storage, and loss modulus; these increased viscoelastic properties of PCS (gel acting behavior) create a great potential for its application in tissue regeneration devices (both as hydrogels and as scaffolds). We also grafted PCS to collagen II and showed its huge impact on the rheological and hence subsequently microstructural, mechanical, and most importantly cell behavior of the scaffolds.

Author statement

Narjes Rashidi: Conceptualization, Methodology, Investigation, Validation, Formal analysis, Writing- Original draft preparation. Jan Czernuszka: Conceptualization, Supervision, Resources, Funding acquisition, Writing- Review & Editing. Maryam Tamaddon: Supervision, Writing- Review & Editing. Chaozong Liu: Supervision, Resources, Funding acquisition.

Declaration of competing interest

The authors declare that they have no known competing financial interests or personal relationships that could have appeared to influence the work reported in this paper.

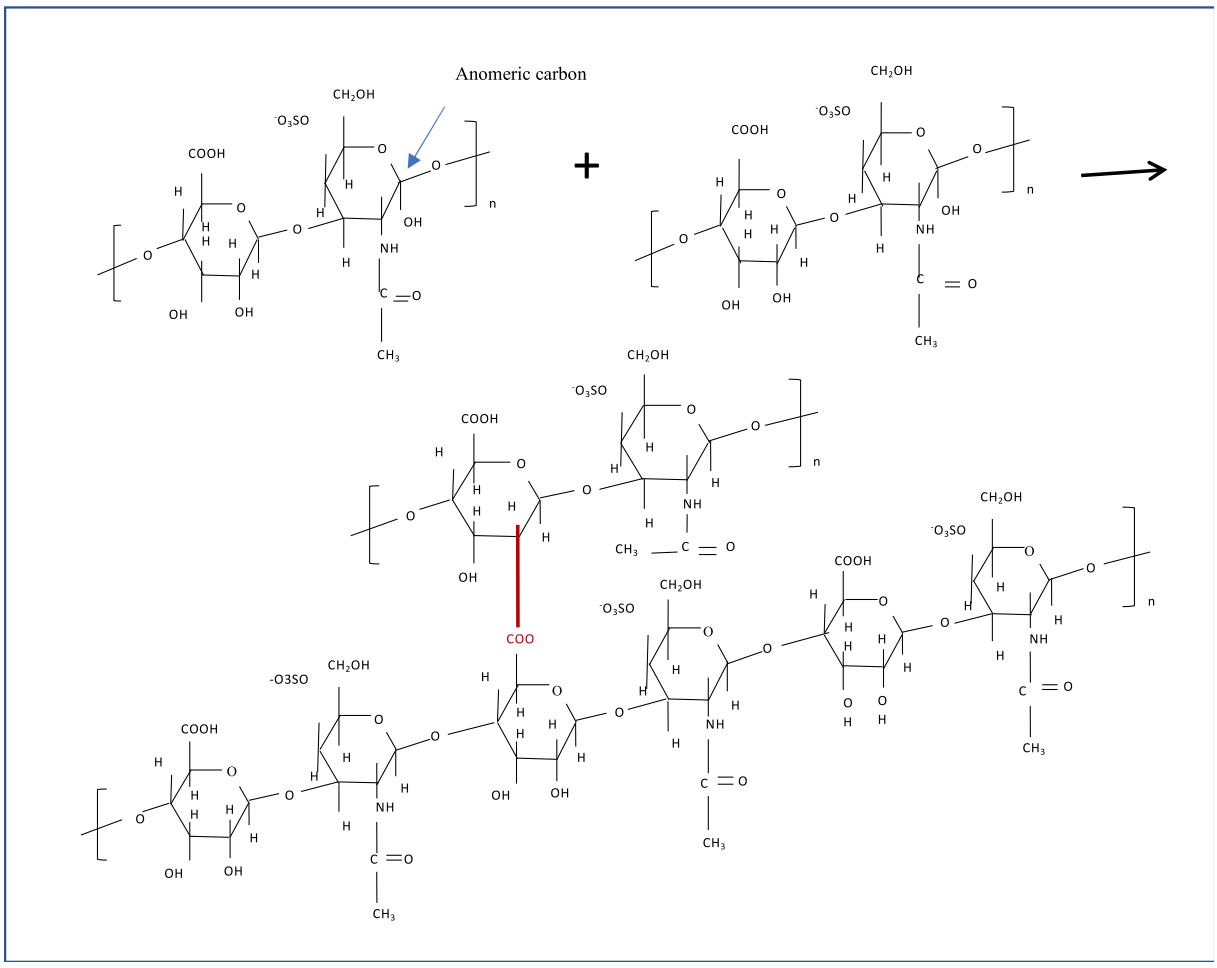

Fig. 7b. Intermolecular chain growth (formation of side branches), through the carboxylate functional group.

Data availability

Data will be made available on request.

Acknowledgments

This work was supported by the Versus Arthritis Research United Kingdom (Grant No. 21977); Innovative United Kingdom via Newton Fund (Grant No. 102872); Engineering and Physical Science Research Council (EPSRC) via the DTP case program (Grant No. EP/T517793/1); National Institute for Health Research (NIHR) via NIHR UCLH BRC-UCL Therapeutic Acceleration Support (TAS) Fund (award no: 180340).

References

[1] J.A. Buckwalter, E.B. Hunziker, Healing of bones, cartilages, tendons, and ligaments: a new era, Lancet 348 (1996) S18.
[2] N.S. Gandhi, R.L. Mancera, The structure of glycosaminoglycans and their interactions with proteins, Chem. Biol. Drug Des. 72 (6) (2008) 455–482.
[3] T. Douglas, S. Heinemann, C. Mietrach, U. Hempel, S. Bierbaum, D. Scharnweber, H. Worch, Interactions of collagen types I and II with chondroitin sulfates AC and their effect on osteoblast adhesion, Biomacromolecules 8 (4) (2007) 1085–1092.
[4] K. Kimata, M. Okayama, A. Oohira, S. Suzuki, Cytodifferentiation and proteoglycan biosynthesis, Mol. Cell. Biochem. 1 (1973) 211–228.
[5] T. Toida, H. Toyoda, T. Imanari, High-resolution proton nuclear magnetic resonance studies on chondroitin sulfates, Anal. Sci. 9 (1993) 53–58.
[6] J.E. Scott, Structure and function in extracellular matrices depend on interactions between anionic glycosaminoglycans, Pathol. Biol. 49 (2001) 284–289.
[7] V.F. Sechriest, Y.J. Miao, C. Niyibizi, A. Westerhausen-Larson, H.W. Matthew, C. H. Evans, F.H. Fu, J.K. Suh, GAG-augmented polysaccharide hydrogel: a novel biocompatible and biodegradable material to support chondrogenesis, Biomed. Mater. Res. 49 (2000) 534–541.
[8] S.J. Bryant, K.A. Davis-Arehart, N. Luo, R.K. Shoemaker, J.A. Arthur, K.S. Anseth, Synthesis and characterization of photopolymerized multifunctional hydrogels: water-soluble poly(vinyl alcohol) and chondroitin sulfate macromers for chondrocyte encapsulation, Macromolecules 37 (18) (2004) 6726–6733.
[9] N.J. Steinmetz, S.J. Bryant, Chondroitin sulfate and dynamic loading alter chondrogenesis of human MSCs in PEG hydrogels, Biotechnol. Bioeng. 109 (10) (2012) 2671–2682.
[10] M. Jin, J. Shi, W. Zhu, H. Yao, D.A. Wang, Polysaccharide-based biomaterials in tissue engineering: a review, Tissue Eng. B 27 (6) (2021) 604–626.
[11] B. Corradetti, F. Taraballi, S. Minardi, J.V. Eps, F. Cabrera, L.W. Francis, S. A. Gazze, M. Ferrari, B.K. Weiner, E. Tasciotti, Chondroitin sulfate immobilized on biomimetic scaffold modulates inflammation while driving chondrogenesis, Stem cells Translat. Med. 5 (5) (2016) 670–682.
[12] S. Chen, W. Chen, Y. Chen, X. Mo, C. Fan, Chondroitin sulfate modified 3D porous electrospun nanofiber scaffolds promote cartilage regeneration, Mater. Sci. Eng. C 118 (2021), 111312.
[13] T. Wang, F. Yang, A comparative study of chondroitin sulfate and heparan sulfate for directing three-dimensional chondrogenesis of mesenchymal stem cells, Stem Cell Res. Ther. 8 (284) (2017).
[14] S. Varghese, N.S. Hwang, A.C. Canver, P. Theprungsirikul, D.W. Lin, J. Elisseeff, Chondroitin sulfate based niches for chondrogenic differentiation of mesenchymal stem cells, Matrix Biol. 27 (1) (2008) 12–21.
[15] M. Tamaddon, R.S. Walton, D.D. Brand, J.T. Czernuszka, Characterisation of freeze-dried type II collagen and chondroitin sulfate scaffolds, J. Mater. Sci. Mater. Med. 24 (5) (2013) 1153–1165.
[16] I. Strehin, Z. Nahas, K. Arora, T. Nguyen, J. Elisseeff, A versatile pH sensitive chondroitin sulfate-PEG tissue adhesive and hydrogel, Biomaterials 31 (10) (2010) 2788–2797.
[17] X. Li, Q. Xu, M. Johnson, X. Wang, J. Lyu, Y. Li, S. McMahon, U. Greiser, A. Sigen, W. Wang, A chondroitin sulfate based injectable hydrogel for delivery of stem cells in cartilage regeneration, Biomater. Sci. 9 (2021) 4139–4148.
[18] I. Goldstein, T. Hullar, Chemical synthesis of polysaccharides, Adv Carbohydr. Chem. 21 (1967) 431–512.
[19] S. Hirano, N. Kashimura, N. Kosaka, K. Onodera, Polysaccharide synthesis from mono-and oligo- saccharides by the action of phosphorus pentoxide in dimethyl sulphoxide, Polymer 13 (5) (1972) 190–194.

[20] P.T. Mora, J.W. Wood, P. Maury, B.G. Young, Synthetic polysaccharides. II. fractionation of Polyglucose1, J. Am. Chem. Soc. 80 (3) (1958) 693–699.
[21] P.H. Seeberger, Solid phase oligosaccharide synthesis, J. Carbohydr. Chem. 21 (7–9) (2002) 613–643.
[22] T. Uryu, Artificial polysaccharides and their biological activities, Prog. Polym. Sci. 18 (4) (1993) 717–761.
[23] M. Faijes, A. Planas, In vitro synthesis of artificial polysaccharides by glycosidases and glycosynthases, Carbohydr. Res. 342 (12) (2007) 1581–1594.
[24] S. Kobayashi, H. Uyama, S. Kimura, Enzymatic polymerization, Chem. Rev. 101 (12) (2001) 3793–3818.
[25] S. Kobayashi, M. Ohmae, Enzymatic polymerization to polysaccharides, Enzyme-catalyzed synthesis of polymers 194 (2006) 159–210.
[26] J. Yang, S. Tsai, J. Chen, C. Yang, Y. Hsieh, Method for Producing Water-Insoluble Polysaccharides, US Patent Documents, 2005.
[27] H. Rennhard, Polysaccharides and their preparation, US Patent 3 (1973), 766,165.
[28] A. Kanazawa, S. Okumura, M. Suzuki, Powder-to-powder polycondensation of natural saccharides. facile preparation of highly branched polysaccharides, Org. Biomol. Chem. 3 (9) (2005) 1746–1750.
[29] N. Rashidi, M. Tamaddon, C. Liu, D.D. Brand, J.T. Czernuszka, A bilayer osteochondral scaffold with self-assembled monomeric collagen type I , type II and polymerized chondroitin sulphate promotes chondrogenic and osteogenic differentiation of mesenchymal stem cells, Adv. NanoBiomed Res. 2 (1) (2021), 2100089.
[30] A. Kanazawa, S. Namiki, M. Suzuki, Thermal polycondensation of sugar fluoride to form highly branched polysaccharide, J. Polym. Sci. Polym. Chem. 45 (17) (2007) 3851–3860.
[31] J.R. Amrutkar, S.G. Gattani, Chitosan–chondroitin sulfate based matrix tablets for colon specific delivery of indomethacin, AAPS PharmSciTech 10 (2) (2009) 670–677.
[32] F.F. Rosloniec, M. Cremer, A.H. Kang, L.K. Myers, D.D. Brand, Collagen-induced arthritis, Curr. Protoc. Im. 89 (15) (2010) 1–25.
[33] J. Armstrong, R. Wenby, H. Meiselman, T. Fisher, The hydrodynamic radii of macromolecules and their effect on red blood cell aggregation, Biophys. J. 87 (6) (2004) 4259–4270.
[34] R. Pamies, J.G.H. Cifre, M.C. López, M&J de la Torre, Determination of intrinsic viscosities of macromolecules and nanoparticles. Comparison of single-point and dilution procedures, Colloid Polym. Sci. 286 (11) (2008) 1223–1231.
[35] P.J. Flory, Principles of Polymer Chemistry, Cornell University Press, 1953.
[36] Å. Wasteson, Properties of fractionated chondroitin sulphate from ox nasal septa, Biochem. J. 122 (4) (1971) 477–485.
[37] G. Harrison, G. Franks, V. Tirtaatmadja, D. Boger, Suspensions and polymers-common links in rheology, Korea-Australia Rheology, Journal 11 (3) (1999) 197–218.
[38] P.J. Daivis, D.J. Evans, G.P. Morriss, Computer simulation study of the comparative rheology of branched and linear alkanes, J. Chem. Phys. 97 (1) (1992) 616–627.
[39] M.A. Cziep, M. Abbasi, M. Heck, L. Arens, M. Wilhelm, Effect of molecular weight, polydispersity, and monomer of linear homopolymer melts on the intrinsic mechanical nonlinearity $^{3}Q_{0}(\omega)$ in MAOS, Macromolecules 49 (9) (2016) 3566–3579.
[40] J. Ding, P.J. Tracey, W. Li, G. Peng, P.G. Whitten, G.G. Wallace, Review on shear thickening fluids and applications, Textiles Light Ind. Sci. Technol. 2 (4) (2013) 161–173.
[41] Å. Wasteson, A method for the determination of the molecular weight and molecular-weight distribution of chondroitin sulphate, J. Chromatogr. A 59 (1) (1971) 87–97.
[42] M.B. Mathews, The molecular weight of sodium chondroitin sulphate by light scattering, Arch. Biochem. Biophys. 61 (2) (1956) 367–377.
[43] E. Sisu, E. Flangea, A. Serb, A.D. Zamfir, Modern developments in mass spectroscopy of chondroitin and dermatan sulfate glycosaminoglycans, Amino Acids 41 (2011) 235–256.
[44] J.P. Gleeson, N.A. Plunkett, F.J. O'Brien, Addition of Hydroxyapatite improves stiffness, interconnectivity and osteogenic potential of highly porous collagen-based scaffold for bone tissue regeneration, Eur. Cell. Mater. 20 (2010) 218–230.
[45] M. Kikuchi, S. Itoh, S. Ichinose, K. Shinomiya, J. Tanaka, Self-organization mechanism in a bone-like hydroxyapatite/collagen nanocomposite synthesized in vitro and its biological reaction in vivo, Biomaterials 22 (13) (2001) 1705–1711.